New insights into the termination of the African Humid Period (5.5 ka BP) in central Ethiopia from detailed analysis of a diatom record

Vincent Roubeix[1] and Françoise Chalié[2]

[1] Irstea, UR RECOVER, Pôle AFB-Irstea hydroécologie plans d'eau, Centre d'Aix en Provence, 3275 route Cézanne, 13182 Aix-en-Provence (France)

email : vincent.roubeix@irstea.fr

[2] Aix-Marseille Université, CNRS, IRD, Coll.France, CEREGE, BP 80, F.13545 Aix-en-Provence (France)

email : chalie@cerege.fr

Keywords : African monsoon; Climate change; Early warning signals; Regime shift; Ecological thresholds

ABSTRACT

The termination of the African Humid Period in northern Africa has been described as abrupt, occurring within centuries, as well as gradual, in response to incremental decreases in summer insolation. This study examined the rapidity of the change in diatom assemblages over the period from 6.5 to 4.5 cal ka BP, in a core studied previously at a coarser resolution. This transition was characterized by high variability of assemblages, which could be related, in part, to changes in water conductivity, and potentially enhanced by a site-specific hydrological threshold or ecological salinity threshold. We hypothesize that the variations in diatom assemblages reflect climate fluctuations, which may have been an early warning signal of an impending climate regime shift.

Introduction

The end of the African Humid Period is one example that shows the Holocene was not characterized by a stable climate (deMenocal and Bond 1997; Gasse 2001). It took place at ca. 5.5 ka BP in north subtropical Africa and gave rise to the Sahara Desert, where there had previously been savanna and lakes for several millennia. Analysis of a marine sediment core near the northwest coast of Africa suggested that this mid-Holocene climate change was abrupt and occurred within centuries (deMenocal et al. 2000). The abruptness of the transition, however, is contradicted by other archives that show more gradual, millennial-scale aridification of the climate (Kröpelin et al. 2008). It seems that rapid termination of the African Humid Period (within 500 years) concerned exclusively the regions of the western Sahara and Eastern Africa (Tierney and deMenocal 2013).

The onset and termination of the African Humid Period is often cited as an example of a regime shift (Scheffer and Carpenter 2003; Walker and Meyers 2004; Seddon et al. 2014). The external trigger was summer solar radiation, which varied continuously following Earth's axis angle and reached a maximum at ca. 9000 years BP. Non-linear responses of precipitation and vegetation were reconstructed as a threshold of insolation was crossed (deMenocal et al. 2000). This radiation threshold was associated with climatic and ecological (through vegetation) positive feedbacks, which accelerated climate change (Tierney and deMenocal 2013).

Paleoclimate indicators can provide information about the timing of the transition from humid to arid conditions in the North African subtropical band. An indicator can show early warning signals that a regime shift is going to occur, in particular through an increase of variance (Wang et al. 2012). Interpretation of a climate proxy, however, may be complicated if it is not linearly related to climate, and if its variations are influenced by site-specific thresholds (Kröpelin et al. 2008).

Analysis of diatoms in a core from Lake Abiyata, Ethiopia, revealed important changes in climate during the Holocene (Gasse 2001; Chalié and Gasse 2002). A striking result was an abrupt increase in diatom-inferred conductivity (lower precipitation-evaporation balance) and a decline in the proportion of planktonic diatoms (shallower lake) around 5.5 ka BP. This suggests rapid (one to a few centuries) aridification of the climate, synchronous with the documented termination of the African Humid Period. Interestingly, a short peak of diatom-inferred conductivity preceded the large increase that marked the beginning of a period of high conductivity. The sampling frequency and indicators that were used, however, were not sufficient for a detailed investigation of this important climate transition.

Lake Abiyata is today a shallow hyper-alkaline lake located in the Ethiopian rift at an elevation of 1600 m. It is part of the endorheic Ziway-Shalla system, composed of four residual lakes. Lake Abiyata receives surface inflow from Lakes Ziway and Langano and has no surface outlet. Its present area is 176 km² and it has an average depth of 7.6 m and a maximum depth of 14.2 m (Ayenew 2007). During the African Humid Period, the four lakes merged to form a single large lake (Gillespie et al. 1983).

The objective of this study was to describe the ecological turnover of diatom assemblages in Lake Abiyata at the end of the African Humid Period and to investigate the information diatoms can provide about lake and climate changes. To this end, additional diatom analyses were undertaken on the core from Lake Abiyata, focusing on the period 6.5 to 4.5 ka BP, so that the transitional state between the African Humid Period and the late Holocene could be quantified climatically.

Materials and methods

Coring and sampling

Sediment core AB95II was collected in 1995 using a Wright corer, in the eastern part of Lake Abiyata (7°35' N; 38°35' E), at a water depth of 7 m. With respect to the section considered here (560-862 cm depth in the core), the sediments were described soon after core opening and splitting, and consisted mainly of a brown, to grey and greenish, organic-rich mud, with a few cm-thick layers of fine sand and cinerite interrupting the mud. Eleven new samples were taken in the core section, adding to the 18 samples analyzed in a previous study (Chalié and Gasse 2002). Each of the 29 samples integrated 1 cm of sediment thickness. Samples were collected at intervals of 2.2 to 24 cm, owing to the lithology, in particular the presence of sand or cinerite layers, and to the availability of well-preserved sediment that remained in the core.

Chronology

We used the sediment chronology developed in a previous study of the core (Chalié and Gasse 2002). The chronological framework was based on radiocarbon dates on bulk organic matter (OM) (Gibert et al. 1999). Ages were considered valid because (1) the OM was shown to be mainly of phytoplankton origin and (2) the ^{14}C activity of the total dissolved inorganic carbon from the modern lake water is in equilibrium with that of atmospheric CO_2. Dates obtained on carbonated material formed at the water-sediment interface showed ages that were too old by 500 to 900 years, probably as a consequence of groundwater inputs that contained dead carbon. These dates were therefore excluded from our chronological framework. The radiocarbon timescale was established

by linear interpolation between adjacent dated levels. The calendar timescale was calibrated with CALIB #4.0 (Stuiver and Reimer 1993; Stuiver et al. 1998; URL address: http://calib.org/calib/).

Three dates were obtained within the depth interval of interest (571.9 to 861.5 cm depth). Two other dates were obtained from sediment samples collected in the core < 25 cm below and above the section considered. These 5 dates were in order between 3900 +/- 90 (551.8 cm depth), and 7100 +/- 80 (885.1 cm depth) ^{14}C years BP. Based on these 5 dates, the mean sedimentation rate was ~0.70 mm a^{-1}, and doubled at ca. 6070 cal a BP to ~1.40 mm a^{-1}, and the chronological framework was considered well constrained during the period of interest. Unless specified otherwise, ages presented in this study are in calendar ka BP.

Sample preparation and diatom enumeration

Organic matter was oxidised with H_2O_2 and carbonates were removed with HCl. Slides were mounted in a high-refractive-index resin (Naphrax©) and observed using light microscopy (magnification x1000). Diatom taxonomy was based on African (Hustedt 1949; Gasse 1986; Cocquyt 1998) and European floras (Krammer and Lange-Bertalot 1986, 1988, 1991a,b).

Conductivity transfer function

The conductivity transfer function used was based on the Weighted Averaging Method (WAM; ter Braak and Loomans 1986; Gasse et al. 1995). The modern reference database used was the African component of the database from the EDDI Program (European Diatom Database Initiative) (Battarbee et al. 2000), hereafter referred to as the modern African dataset. Details of the methods can be found in Chalié and Gasse (2002). In the latter study, past pH and ionic ratios were also inferred for Lake Abiyata using other transfer functions, but it was shown that their variations were

highly correlated to conductivity. The present study therefore focused on conductivity, which is also the variable most directly related to the precipitation-evaporation balance and climate change. Two notable sources of uncertainty in the transfer function are: (1) the difference in temporal integration of water samples and diatom sediment samples in the training dataset (especially for lakes having high seasonal variability), and (2) interactions between potential confounding factors (Juggins 2013). The transfer function was applied here, however, in its field of calibration and its performance with respect to water conductivity reconstruction (Gasse et al 1995) suggests that such uncertainties are minimal. Most of the species present in the core section of interest were included in the transfer function (90%).

Data analysis

All data analyses were performed with R (R Core Team 2016). Correspondence analysis (CA) was applied to species relative abundance data to show variations in diatom assemblages through time. Only species having a maximum relative abundance in the sequence greater than 2 % were considered (n=28). Sample coordinates in each of the three main dimensions of CA (CA1, CA2 and CA3) were plotted against sample age estimated from the core age model. Groups identified in the CA were characterized by indicator species, determined by IndVal analysis using the labdsv R package (David 2016).

Individual species relationships to water conductivity were examined using the modern African dataset. Moreover, the responses to the conductivity gradient of all species present in the dataset were evaluated through a single gradient forest analysis. Gradient forest is a machine learning method to extract ecological community thresholds from the crossing of species and environment tables. It is a kind of breakpoint analysis that considers many species and environmental variables together. It is based on the development of a random forest for each species

and the analysis of data splits produced by all specific models on every environmental gradient (Ellis et al. 2012; Roubeix et al. 2016). In addition to threshold detection, gradient forest estimates the relative importance of environmental variables in species distribution among sites. Log-transformed diatom species relative abundances in the sediment samples of the modern African dataset were considered for the analysis. Five hydrochemical variables were used to run the analysis: pH, alkalinity, conductivity, anion $(HCO_3^-+CO_3^-)/(Cl^-+SO_4^{2-})$ and cation $(Na^++K^+)/(Ca^{2+}+Mg^{2+})$ ratios. Their correlations in the dataset were moderate (<0.5 Spearman), except between conductivity and alkalinity (0.53), alkalinity and cation ratio (0.56), and conductivity and anion ratio (-0.69). Potential thresholds identified by gradient forest were considered in the conductivity gradient.

Results

The application of the conductivity transfer function to the sediment samples collected in the time interval 6.5 to 4.5 ka BP shows that there was a second sharp increase in conductivity after the short peak at 5.7 ka BP (Fig. 1). This increase at ca 5.3 ka BP was followed by a period of relatively stable and high conductivity until 4.5 ka BP. When reconstructed water conductivity is considered alone, the change in lake chemistry appears rather abrupt if one omits the single peak at 5.7 ka BP. The CA on diatom assemblages, however, reveals a transition period between two relatively stable states (Fig. 2). This transition period lasted approximately 600 years, and was characterized by important variations through time of the diatom assemblages, as shown by the distance between successive samples in the plot formed by the two major dimensions of the CA (34% + 24% = 58 % eigenvalue). The indicator species of the group of samples preceding the transition belong mostly to the genera *Fragilaria* and *Stephanodiscus* (Table 1). Among the indicator species that characterize the samples following the transition are two with high IndVal values: *Anomoeoneis sculpta* and

Rhopalodia gibberula. During the transition period, one sample comes very close to the later stable group (Fig. 2).

The turnover of diatom assemblages along CA1 is very similar to the plot of diatom-inferred conductivity (Figs. 1 and 2b). This means that CA1 is related to the abundance of the main indicator species of high conductivity (e.g. *Anomoeoneis sculpta*). It appears clearly that the two stable groups of samples correspond to two successive states of the lake, with low and then high water conductivity. The sample of the first group that appears close to the second group in the CA plot is at the top of a very narrow peak of conductivity, reaching the level of the latest samples of the studied sequence (Fig. 2b). Along CA2, the diatom assemblage variations during the transition period are not correlated to inferred changes in conductivity. Variability between the two stable states is strongly enhanced, with up and down variations extending beyond the interval between the initial and final states. The pattern is similar along CA3, although the coordinates of the two stable states are almost equal and the variability is a bit lower. Regarding variations in CA2, four consecutive lows can be identified in respect to a basal level close to the one prevailing at the end of the sequence. The two species that most contribute to CA2 are *Rhopalodia gibberula* and *Stephanodiscus minutulus* (Fig. 3). The three first lows of CA2 correspond to peaks in relative abundance of *S. minutulus* and *R. gibberula*, whereas the fourth low is associated with a high relative abundance of *R. gibberula*.

The peak of inferred conductivity is a consequence of high variations in relative abundance of several species (Fig. 4). The species *Rhopalodia gibberula* and *Anomoeoneis sculpta* had much higher relative abundance at the peak, whereas the relative abundances of *Rhopalodia gibba* and *Stephanodiscus astraea* were much lower. Each of these species had a similar relative abundance just before and after the peak. The distributions of the four species along the conductivity gradient of the modern African dataset reveal a zone in the gradient between 3 and 3.5 where the relative abundance of every species is lowest or changes abruptly (Fig. 5). Indeed, this common threshold

appears like an approximate upper limit of conductivity for *R. gibba* and a lower limit for *R. gibberula* and *A. sculpta*. The species *S. astraea* is abundant at conductivities either lower or higher than the threshold. The analysis of the modern African dataset by gradient forest (Fig. 6) showed that (1) conductivity was the most important predictor among the five hydrochemical variables, (2) samples were uniformly distributed in the conductivity gradient, and (3) there was a clear peak of split density around 3.2 (log µS cm^{-1}). This peak indicates a critical zone in the gradient with maximal turnover of diatom communities.

Discussion

When the whole Holocene sediment core from Lake Abiyata is considered (Gasse 2001; Chalié and Gasse 2002), the conspicuous jump in diatom-inferred conductivity at 5.3 ka BP may be interpreted as a rapid change in climate (within a few decades), having immediate repercussions on lake hydrochemistry. The short peak preceding the period of higher conductivity is almost undetectable over such a large time scale. Reports of rapid and synchronous climate changes from coastal sediments in northwest and eastern Africa (deMenocal et al. 2000; Tierney and deMenocal 2013), however, motivated a detailed investigation of this critical period in sediments of Lake Abiyata. There are regional differences in the termination of the African Humid Period across the continent (Burrough and Thomas 2013). Lake Abiyata lies between the Gulf of Aden and Lake Turkana, where paleoclimate records showed rapid, century-scale change to a drier climate (Fig. 1) (Tierney and deMenocal 2013). The detailed analysis of diatom assemblages, with the addition of supplementary samples in the sediment core, yielded evidence of a rapid climate transition at this site, synchronous with other studies.

Focusing on the period 6.5 to 4.5 ka BP, the change in diatom-inferred conductivity appears less abrupt and the single peak preceding the final rise suggests a transition period was already

under way. Inferred conductivity, however, seems to represent only a moderate part of the variation in diatom assemblage composition, judging from the high correlation of inferred conductivity with CA1 (34 % eigenvalue, Fig. 2). The identification of the transition period between two relatively stable states mainly comes from the variations along CA2. This second dimension shows modifications of diatom assemblages that are not linked to major changes in water conductivity, but likely to other limnological factors influenced by climate, such as water level (P-E balance), mixing (related to temperature and depth), turbidity or nutrient input (via precipitation and erosion). The first stable state is characterized by small planktonic species, and the second stable state is defined by the importance of large, benthic, salt-tolerant species such as *Anomoeoneis sculpta* or *Rhopalodia gibberula* (Table 1). These two states correspond to a deep, freshwater lake and a shallow saline lake, respectively. The estimated duration of the transition period (<600 years) is consistent with an abrupt termination of the African Humid Period, as recorded in the Gulf of Aden and Lake Turkana (Tierney and deMenocal 2013).

The short peak along CA1 and the regular oscillations along CA2 suggest high variability in the lake during the transition period. The two species, *S. minutulus* and *R. gibberula*, which are most related to CA2, may be associated with intermediate states of the lake. Successive dominance of a planktonic species (*S. minutulus*) and a benthic species (*R. gibberula*) at peaks in CA2 is consistent with a trend of decreasing water level, but with several reversals. The termination of the African Humid Period was considered a climate regime shift triggered by a gradual decrease in solar irradiance (deMenocal et al. 2000; Foley et al. 2003). A regime shift is likely to be indicated by changes in system dynamics, which can be considered early warning signals (Thomas 2016). A review of eight past climate transitions revealed that most of them were preceded by early warning signals that could be detected statistically in paleoecological time series (Dakos et al. 2008). One of these transitions was North African desertification. Dakos et al. (2008) noticed an increase in autocorrelation before the transition, which is one early warning sign that indicates the system is

slowing down. An increase of variance can be also a sign that a system is losing stability and approaching a tipping point (Thomas 2016). During the transition period, the climate in Ethiopia may have switched between alternative, i.e. arid and humid states. The Lake Abiyata diatom communities probably recorded flickering of the climate before the regime shift. As underlined by Wang et al. (2012), increased variance may be an early warning signal, even in a low-resolution record, but with a constant sampling frequency along the sequence (Carstensen et al. 2013). In this study, the increase in variance observed during the transition is not associated with a higher sampling frequency and is therefore not an artefact.

The short peak of inferred conductivity is a prominent feature of the transition recorded in the sequence. As it is formed by a single sample, its climatic meaning is dubious. This sample, however, may be significant for several reasons. First, sediment reworking would lead to older sediment from the large freshwater lake being re-deposited in the context of a low-stage, saline lake, rather than the contrary. Second, a similar and synchronous peak of diatom-inferred conductivity (a single sample) was recorded in neighboring Lake Tilo at ca. 4800 ^{14}C a BP (Telford and Lamb 1999). And last, the independent variations of CA2 suggest that rapid lake fluctuations were possible during this transition period. The peak in conductivity (or CA1) may be one additive expression of the variability observed in CA2 during the transition.

The question of how the lake water could have reached such high conductivity and returned to a low-salinity condition in only a few decades, remains (Fig. 1). Two possible, non-exclusive explanations for this single peak can be provided, both implying a threshold effect, which enhanced lake response to climate oscillations. First, the lake had probably already decreased in volume substantially by this time and had therefore become responsive to changes in precipitation-evaporation balance. Variations in water conductivity may have been accentuated by a water-level threshold, below which there was no outflow from the lake (a terminal lake) and salts concentrated faster. Subtle fluctuations around such a threshold may have produced large variations in

conductivity. The hypothesis of such a site-specific threshold effect was also proposed to explain the rapid freshwater-to-saline transition recorded in the sediments of Lake Yoa at 4 ka BP (Kröpelin et al. 2008). For the case of Lake Abiyata, hydrological simulations could provide insights into the possibility of such a rapid conductivity change, reconstructed from diatoms.

The other explanation is the existence of an ecological salinity threshold for diatoms. In this case, a modest salinity increase above a threshold would imply an important change in diatom community composition that could have been reversed when conductivity once again fell below the threshold. The conductivity transfer function based on weighted averaging (Gasse et al. 1995; Chalié and Gasse 2002) could thus have exaggerated the amplitude of salinity change. More investigations are needed on the potential effect of ecological thresholds on inferences derived from transfer functions, especially with regard to the number of species involved and their specific tolerances. The main conductivity threshold may be around 3.2 (1600 µS cm^{-1}), as suggested by diatom species distributions in the conductivity gradient of the modern African dataset (Fig. 6). Approximately the same ecological threshold emerged when all species in the dataset were considered (via gradient forest) and when only the four species most associated with the conductivity peak were considered. This suggests an ecological significance of this threshold. The correlations between variables in the modern African dataset, however, suggest that pH or ionic composition could contribute to this threshold. The species *Stephanodiscus astraea* exhibits relatively high abundance on either side of the gradient. This suggests that two different ecotypes might have been included in the same morphotype. The threshold identified in this study is close to the freshwater-oligohaline limit generally accepted for saline lakes using ecological or physiological criteria (Hammer 1986).

Conclusions

Although the time resolution was low, the diatom record from Lake Abiyata revealed interesting features about the termination of the African Humid Period in Ethiopia. A transition period was clearly delimited from variations in diatom assemblages. Its duration was estimated to be < 600 years and it may correspond to a period of climate transition characterized by high climate variability (rainfall). The variations in diatom assemblages suggest climate oscillations whose effect on the lake may have been enhanced by site-specific or ecological thresholds. These oscillations may represent early warning signals that preceded the climate regime shift to arid conditions. The termination of the African Humid Period may not have been a progressive drop in monsoon intensity as suggested by low-resolution oceanic records that integrate information over large areas. In central Ethiopia, it was instead a period of humid climate interrupted by severe droughts that probably had catastrophic effects on terrestrial ecosystems and human populations as early as 5.8 ka BP.

Acknowledgements

We thank Jean-Charles Mazur (CEREGE) for slide preparation of the new analyzed samples. Sediment core samples were collected under the auspices of CNRS-INSU Programs PNEDC-ERICA (‘Environmental Research for Intertropical Climate in Africa’, R.Bonnefille, coord.), and ECLIPSE-CLEHA (‘CLimat, Environnement et dynamique des populations Humaines en Afrique de l’Est depuis 20,000 ans’, D.Williamson coord.). We are grateful to Keely Mills for valuable comments and suggestions that greatly improved the manuscript, and to an anonymous reviewer for helpful comments.

References

1 Ayenew T (2007) Water management problems in the Ethiopian rift: Challenges for development. J
2 African Earth Sci 48:222-236

3 Battarbee R, Juggins S, Gasse F, Erson NJ, Bennion H, Cameron NG (2000) European Diatom
4 Database Initiative (EDDI), http://craticula.ncl.ac.uk/Eddi/jsp/index.jsp

5 Burrough SL, Thomas DSG (2013) Central southern Africa at the time of the African Humid Period:
6 a new analysis of Holocene palaeoenvironmental and palaeoclimate data. Quaternary Sci Rev
7 80:29-46

8 Carstensen J, Telford RJ, Birks HJB (2013) Diatom flickering prior to regime shift. Nature 498:E11

9 Chalié F, Gasse F (2002) Late Glacial-Holocene diatom record of water chemistry and lake level
10 change from the tropical East African Rift Lake Abiyata (Ethiopia). Palaeogeogr Palaeoclimatol
11 Palaeoecol 187:259-283

12 Cocquyt C (1998) Diatoms from the Northern Basin of Lake Tanganyika. Bibliotheca Diatomologica
13 39, Stuttgart, 275 pp

14 Dakos V, Scheffer M, van Nes EH, Brovkin V, Petoukhov V, Held H (2008) Slowing down as an early
15 warning signal for abrupt climate change. Proc Natl Acad Sci USA 105:14308-14312

16 David WR (2016) labdsv: Ordination and Multivariate Analysis for Ecology. R package version 1.8-0
17 https://CRAN.R-project.org/package=labdsv

18 deMenocal P, Bond G (1997) Holocene climate less stable than previously thought. Eos, Trans Am
19 Geophys Union 78:447-454

20 deMenocal P, Ortiz J, Guilderson T, Adkins J, Sarnthein M, Baker L, Yarusinsky M (2000) Abrupt
21 onset and termination of the African Humid Period: rapid climate responses to gradual insolation
22 forcing. Quaternary Sci Rev 19:347-361

Ellis N, Smith SJ, Pitcher CR (2012) Gradient forests: calculating importance gradients on physical predictors. Ecology 93:156-168

Foley JA, Coe MT, Scheffer M, Wang GL (2003) Regime shifts in the Sahara and Sahel: Interactions between ecological and climatic systems in northern Africa. Ecosystems 6:524-539

Gasse F (1986) East African diatoms: Taxonomy, Ecological Distribution. Bibliotheca Diatomologica 11. Cramer, Berlin, 201 pp

Gasse F (2001) Paleoclimate- Hydrological changes in Africa. Science 292:2259-2260

Gasse F, Juggins S, Ben Khelifa L (1995) Diatom-Based Transfer-Functions for Inferring Past Hydrochemical Characteristics of African Lakes. Palaeogeogr Palaeoclimatol Palaeoecol 117:31-54

Gibert E, Travi Y, Massault M, Chernet T, Barbecot F, Laggoun-Defarge F (1999) Comparing carbonate and organic AMS-C-14 ages in Lake Abiyata sediments (Ethiopia): Hydrochemistry and paleoenvironmental implications. Radiocarbon 41:271-286

Gillespie R, Street-Perrott FA, Switsur R (1983) Post-Glacial arid episodes in Ethiopia have implications for climate prediction. Nature 306:680-683

Juggins S (2013) Quantitative reconstructions in palaeolimnology: new paradigm or sick science? Quaternary Sci Rev 64:20-32

Hammer UT (1986) Saline Lake Ecosystems of the World. Monographiae Biologicae, XI, Springer Netherlands, 616 pp

Hustedt F (1949) Exploration du Lac National Albert: Süsswasser Diatomen aus dem Albert-National Park in Belgisch-Kongo. Mission H. Damas (1935-36), Brussels, 199 pp

Krammer K, Lange-Bertalot H (1986-88-91a,b) Süsswasserflora von Mitteleuropa: Bacillariophyceae, 1-4, Gustav Fischer Verlag, Jena

Kröpelin S, Verschuren D, Lezine AM, Eggermont H, Cocquyt C, Francus P, Cazet JP, Fagot M, Rumes B, Russell JM, Darius F, Conley DJ, Schuster M, von Suchodoletz H, Engstrom DR (2008) Climate-driven ecosystem succession in the Sahara: The past 6000 years. Science 320:765-768

R Core Team (2016). R: A language and environment for statistical computing. R Foundation for Statistical Computing, Vienna, Austria. URL https://www.R-project.org/

Roubeix V, Danis PA, Feret T, Baudoin JM (2016) Identification of ecological thresholds from variations in phytoplankton communities among lakes: contribution to the definition of environmental standards. Environ Monit Assess 188: 246. https://doi.org/10.1007/s10661-016-5238-y

Scheffer M, Carpenter SR (2003) Catastrophic regime shifts in ecosystems: linking theory to observation. Trends Ecol Evol 18:648-656

Seddon AWR, Froyd CA, Witkowski A, Willis KJ (2014) A quantitative framework for analysis of regime shifts in a Galapagos coastal lagoon. Ecology 95:3046-3055

Stuiver M, Reimer PJ (1993) Extended C-14 Data-Base and Revised Calib 3.0 C-14 Age Calibration Program. Radiocarbon 35:215-230

Stuiver M, Reimer PJ, Bard E, Beck JW, Burr GS, Hughen KA, Kromer B, McCormac G, Van der Plicht J, Spurk M (1998) INTCAL98 radiocarbon age calibration, 24,000-0 cal BP. Radiocarbon 40:1041-1083

Telford RJ, Lamb HF (1999) Groundwater-mediated response to Holocene climatic change recorded by the diatom stratigraphy of an Ethiopian crater lake. Quaternary Res 52:63-75

ter Braak CJF, Looman CWN (1986) Weighted averaging, logistic regression and the Gaussian response model. Vegetatio 65:3-11

1 Thomas ZA (2016) Using natural archives to detect climate and environmental tipping points in the
2 Earth System. Quaternary Sci Rev 152:60-71

3 Tierney JE, deMenocal PB (2013) Abrupt shifts in horn of Africa hydroclimate since the Last Glacial
4 Maximum. Science 342:843-846

5 Walker B, Meyers JA (2004) Thresholds in ecological and social-ecological systems: a developing
6 database. Ecol Soc 9(2)

7 Wang R, Dearing JA, Langdon PG, Zhang EL, Yang XD, Dakos V, Scheffer M (2012) Flickering
8 gives early warning signals of a critical transition to a eutrophic lake state. Nature 492:419-422

9

Table 1 List of indicator species in the groups of samples before (group 1) and after (group 2) the climate transition, with their indicator value (IndVal) and p values from significance test, and their conductivity optima and tolerance in the transfer function

Species	Group	IndVal	p value	Conductivity Optimum (log µS cm^{-1})	Tolerance (log µS cm^{-1})
Amphora pediculus (Kützing) Grunow	1	0.84	0.001	2.73	0.37
Cocconeis thumensis A.Mayer	1	0.38	0.041	1.84	0.6
Fragilaria brevistriata Grunow	1	0.79	0.001	2.76	0.8
Fragilaria capucina Desmazieres	1	0.5	0.01	2.53	0.34
Fragilaria construens (Ehrenberg) Grunow f. construens	1	0.84	0.002	2.71	0.72
Fragilaria zeilleri Héribaud	1	0.75	0.001	3.03	0.7
Navicula seminuloides Hustedt in A. Schmidt	1	0.63	0.035	2.99	0.98
Nitzschia amphibia Grunow f. rostrata Hustedt	1	1	0.001		
Nitzschia epiphytica O.Muller	1	0.82	0.001	2.44	1.03
Stephanodiscus astraea (Ehrenberg) Grunow	1	0.95	0.001	2.67	1.03
Stephanodiscus medius Håkansson	1	0.99	0.001	2.67	1.03
Anomoeoneis sculpta (Ehrenberg) Cleve	2	1	0.001	4.23	0.43
Amphora veneta Kützing	2	0.64	0.018	3.06	0.64
Aulacoseira granulata (Ehrenberg) Simonsen	2	0.55	0.034	2.14	0.46
Nitzschia amphibia Grunow f. amphibia	2	0.5	0.043	2.66	0.75
Rhopalodia gibberula (Ehrenberg) O.Muller	2	0.99	0.001	3.91	0.46
Surirella ovalis Brebisson	2	0.64	0.018	3.18	0.78

Fig. 1 The termination of the African Humid Period in East Africa through hydroclimate proxies in Holocene sediment records. (**a**) Hydrogen isotope composition of leaf waxes in a core from the Gulf of Aden (from Tierney and deMenocal 2013), (**b**) diatom-inferred conductivity of Lake Abiyata (from Chalié and Gasse 2002), (**c**) same data with a focus on the period from 6.5 to 4.5 cal ka BP and addition of new samples (empty circles) and (**d**) location of the Zwai-Shalla lake system including Lake Abiyata. The dashed line represents the shoreline of the middle Holocene Lake and the star indicates the coring site.

Fig. 2 Correspondence analysis of diatom samples from the period 6.5 to 4.5 cal ka BP. Representation of the samples in the two first dimensions with % eigenvalue barplot (**a**) and variations through time in the first (CA1, 34% [**b**]), second (CA2, 24% [**c**]) and third (CA3, 12% [**d**]) dimensions. Groups 1 and 2 correspond to the samples before and after the transition period, respectively. The grey band represents the transition period with higher variability of the assemblages; its time limits are given by the estimated dates for the latest sample in group 1 (5821 cal a BP) and the first sample in group 2 (5229 cal a BP). The maximum duration of the transition period is therefore estimated about 600 years

Fig. 3 Variations through time in relative abundance of the two diatom species, *Rhopalodia gibba* and *Stephanodiscus minutulus*, which contribute most to the second axis of the correspondence analysis (CA2) as shown by the barplot of species contributions

Fig. 4 Relative abundance of the four diatom species *Rhopalodia gibba*, *Stephanodiscus astraea*, *Rhopalodia gibberula* and *Anomoeoneis sculpta*, showing the largest variations among the three consecutive sediment samples forming the diatom-inferred conductivity peak before 5.5 cal ka BP. Dates were estimated using the core age model (Chalié and Gasse 2002)

Fig. 5 Relative abundance of the species *Rhopalodia gibba*, *Stephanodiscus astraea*, *Rhopalodia gibberula* and *Anomoeoneis sculpta* in the conductivity gradient of the modern African diatom dataset. The grey band indicates a potential community threshold

Fig. 6 Result of gradient forest analysis on the modern African diatom dataset. The barplot in the top left corner represents the relative importance of the five hydrochemical variables used in the analysis (Cond = conductivity, Alk = alkalinity). The lines in the graph are the density of splits (i.e. breakpoints) in the conductivity gradient (black line), the density of data (dashed line) and the ratio of densities (grey line). The peaks of the ratio of densities indicate potential ecological community thresholds

1 **Fig. 1**

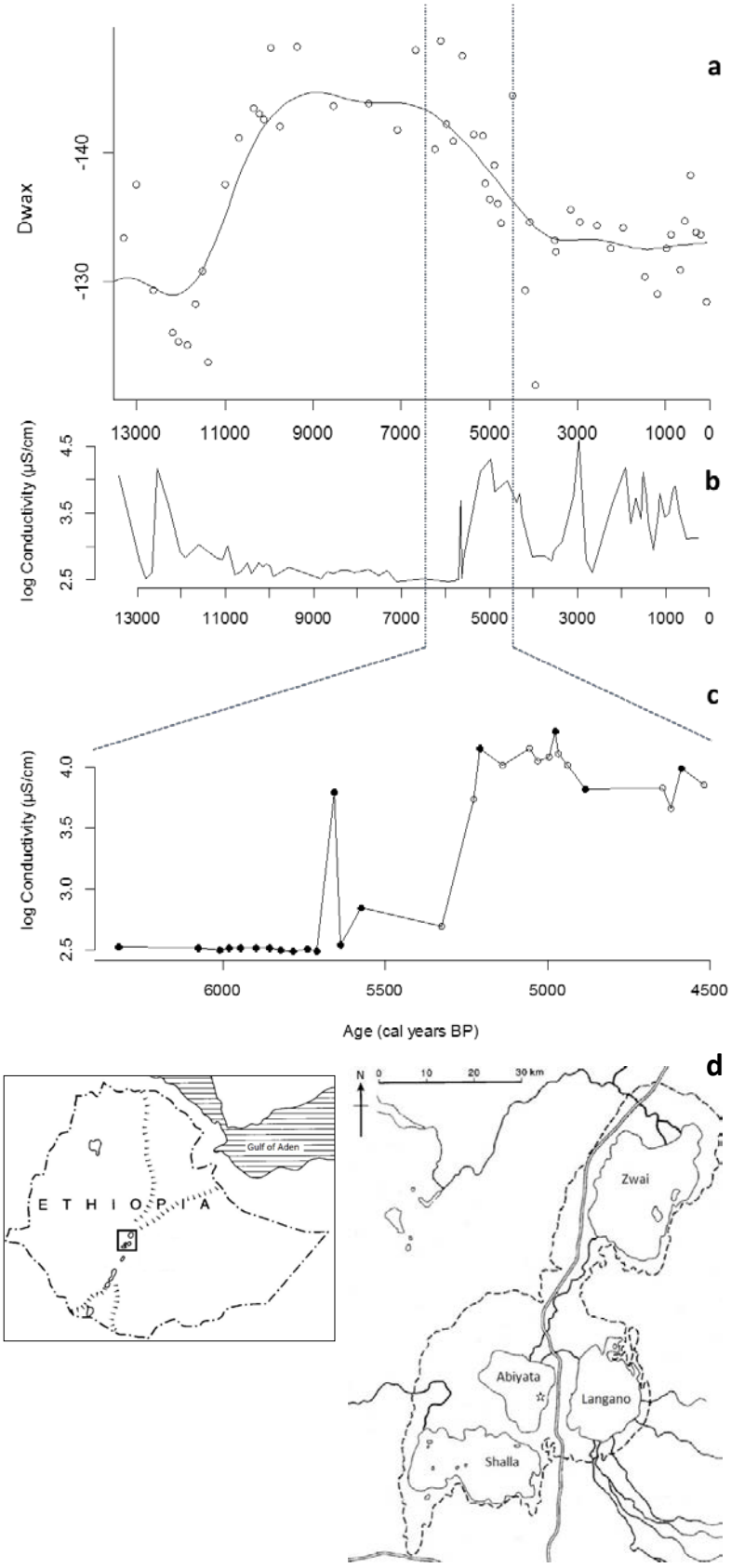
a
Dwax
-140
-130
13000
11000
9000
7000
5000
3000
1000
0
b
log Conductivity (µS/cm)
4.5
3.5
2.5
c
4.0
3.0
6000
5500
5000
4500
Age (cal years BP)
d
N
0
10
20
30 km
Gulf of Aden
E T H I O P I A
Zwai
Abiyata
Langano
Shalla

2

1 **Fig. 2**

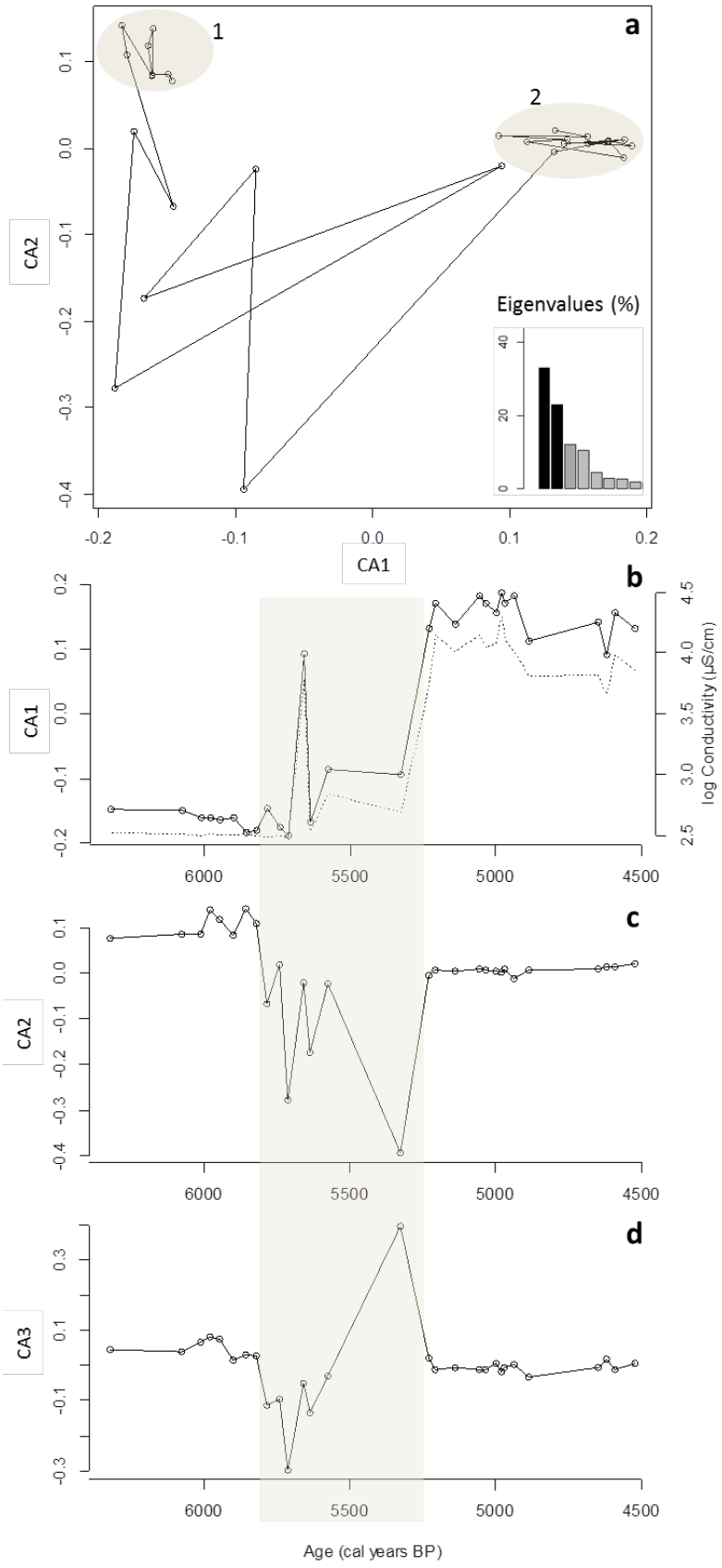
a
1
2
CA2
CA1
Eigenvalues (%)
b
CA1
log Conductivity (µS/cm)
c
CA2
d
CA3
Age (cal years BP)

2

1 **Fig. 3**

2

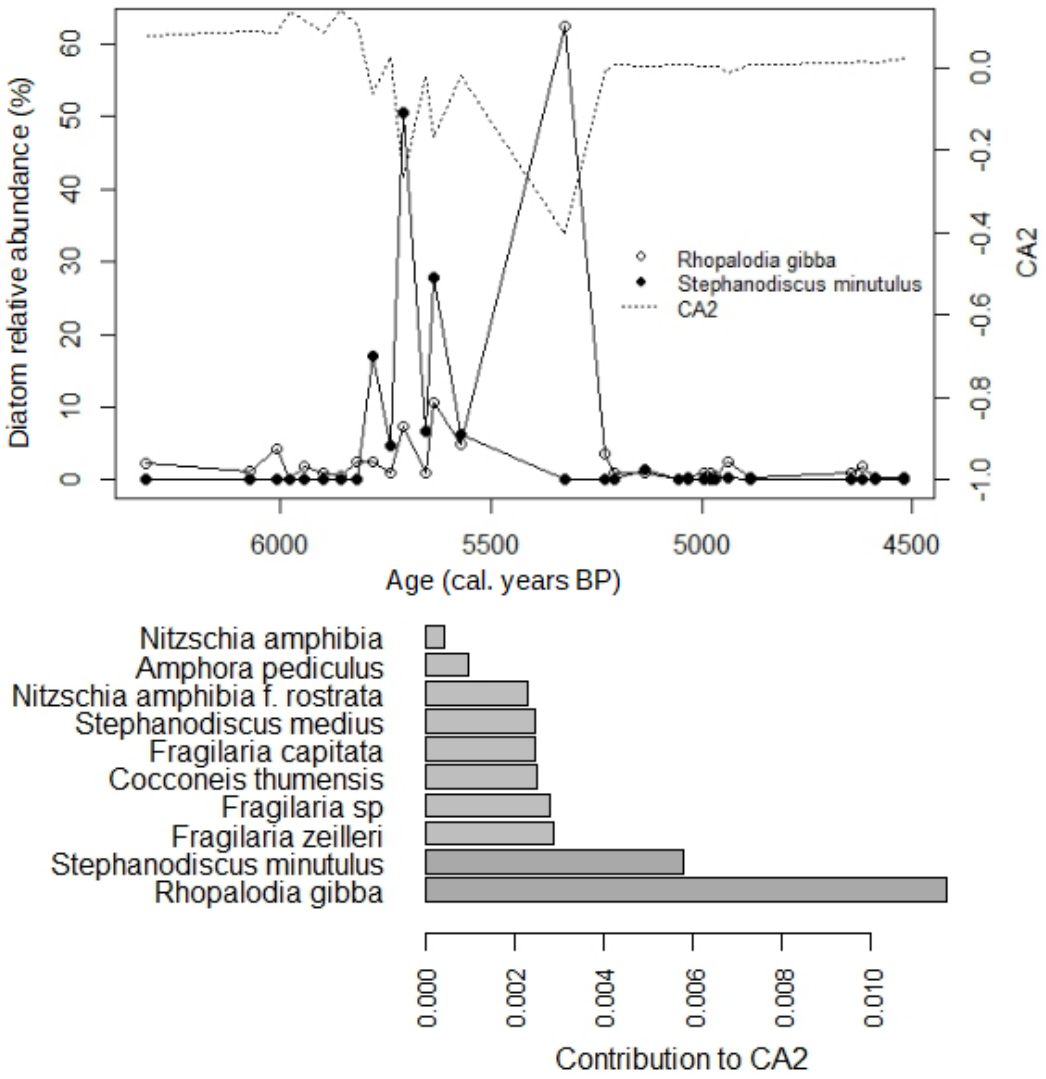
Diatom relative abundance (%)
0
10
20
30
40
50
60
6000
5500
5000
4500
Age (cal. years BP)
Rhopalodia gibba
Stephanodiscus minutulus
CA2
0.0
-0.2
-0.4
-0.6
-0.8
-1.0
CA2
Nitzschia amphibia
Amphora pediculus
Nitzschia amphibia f. rostrata
Stephanodiscus medius
Fragilaria capitata
Cocconeis thumensis
Fragilaria sp
Fragilaria zeilleri
Stephanodiscus minutulus
Rhopalodia gibba
0.000
0.002
0.004
0.006
0.008
0.010
Contribution to CA2

Fig. 4

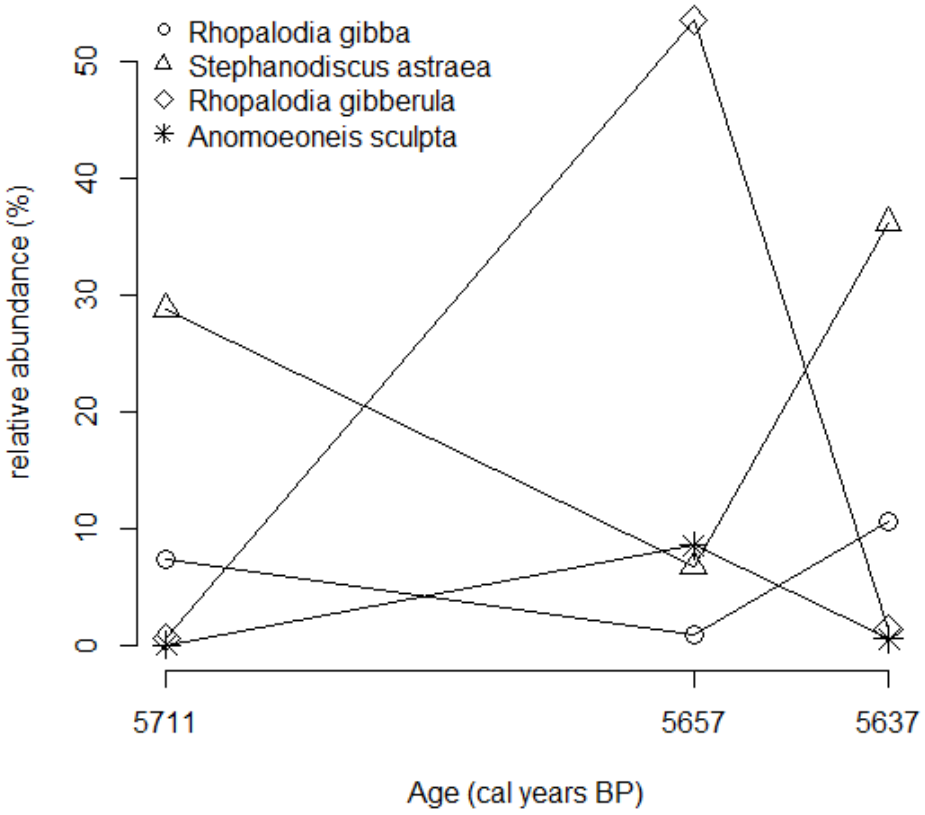
Rhopalodia gibba
Stephanodiscus astraea
Rhopalodia gibberula
Anomoeoneis sculpta
relative abundance (%)
0
10
20
30
40
50
5711
5657
5637
Age (cal years BP)

Fig. 5

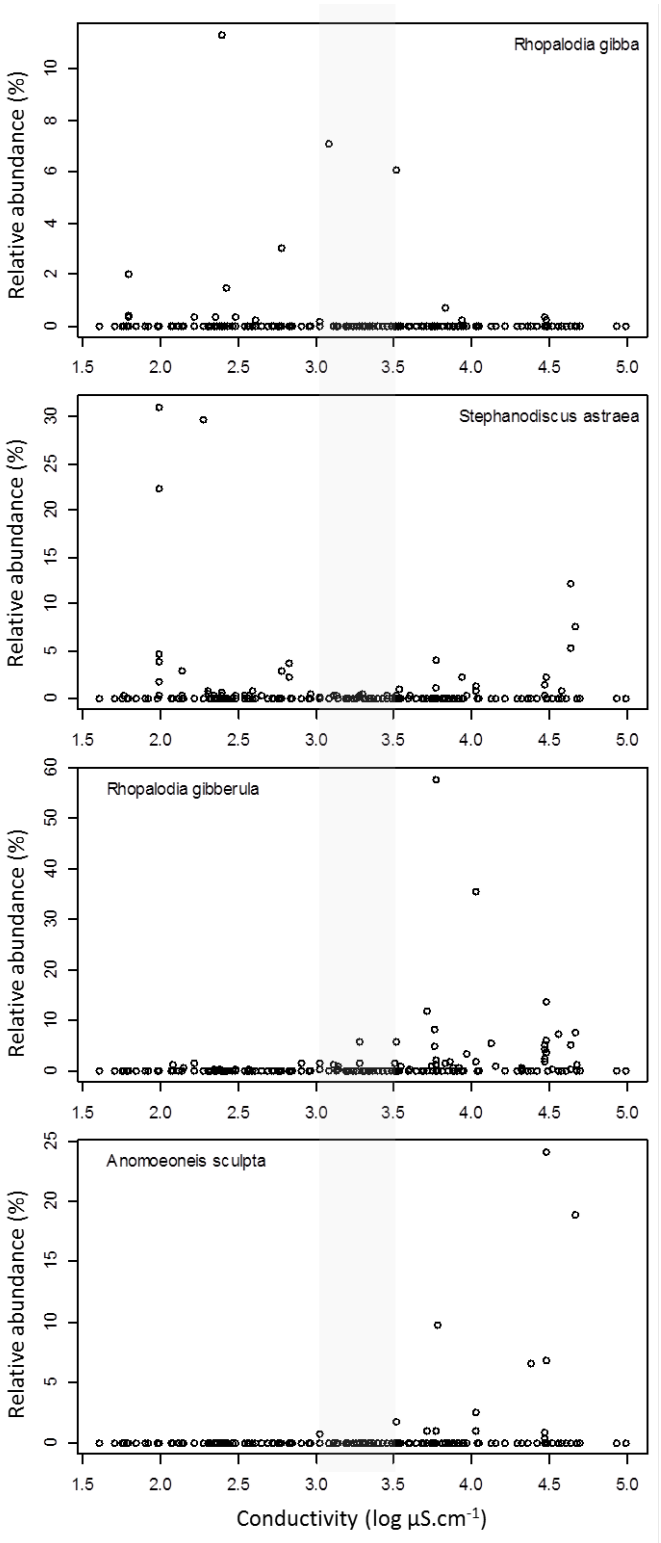
Rhopalodia gibba
Stephanodiscus astraea
Rhopalodia gibberula
Anomoeoneis sculpta
Relative abundance (%)
Conductivity (log µS.cm-1)

Fig. 6

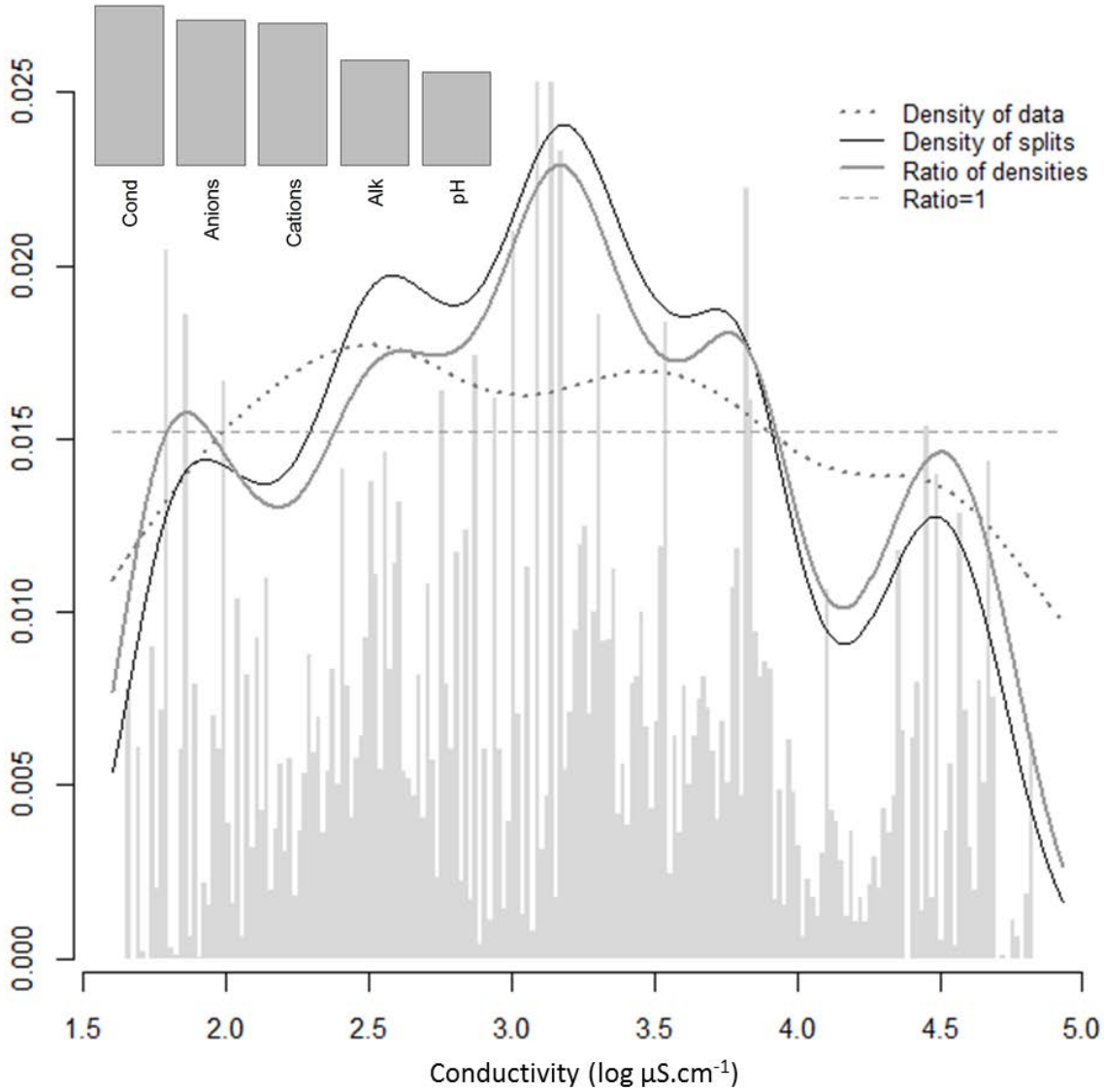
Cond
Anions
Cations
Alk
pH
Density of data
Density of splits
Ratio of densities
Ratio=1
0.000
0.005
0.010
0.015
0.020
0.025
1.5
2.0
2.5
3.0
3.5
4.0
4.5
5.0
Conductivity (log µS.cm-1)